Brazilian Journal of Botany (2020) 43:81–89
https://doi.org/10.1007/s40415-020-00590-y

ORIGINAL ARTICLE

Analysis of flavonoids and anthocyanin biosynthesis-related genes expression reveals the mechanism of petal color fading of *Malus hupehensis* (*Rosaceae*)

Meiling Han[1] · Chen Yang[1] · Jing Zhou[1] · Jiabin Zhu[1] · Jiaxin Meng[1] · Ting Shen[1] · Zhuanxia Xin[1] · Houhua Li[1]

Received: 30 October 2019 / Revised: 6 February 2020 / Accepted: 8 February 2020 / Published online: 3 March 2020

Abstract

Malus hupehensis (Pamp.) Rehder is an indigenous wild crabapple tree from China that has received increased attention, due to its significant ornamental and economical values. The flowers change from red to white during development, a phenomenon that is prevalent within *Malus* genus. However, there are no reports on the phytochemical aspects of *M. hupehensis* flower. Here, we investigated the mechanism of color fading through biochemical and molecular analysis of *M. hupehensis* petals during development. Sixteen flavonoids were detected, and cyanidin-3-galactoside was the major anthocyanin in petals. The levels of most compounds initially increased and then decreased during flower development. The changing profile of total anthocyanins was consistent with the changes in floral color. Analysis of anthocyanin biosynthesis-related genes showed that the expression levels of *PAL*, *CHS*, *CHI*, *DFR*, *FLS*, *ANS*, *UFGT*, *MYB10* and *MYB12* were significantly higher at early stages than at later stages, similarly to the change in cyanidin-3-galactoside contents. *MYB10* and *MYB12* significantly positively correlated with *CHS*, *CHI* and *DFR*. There was a particularly strong positive correlation between *MYB10* and *ANS*, and *MYB12* was strongly positively correlated with *LAR*. Thus, *MYB10* appeared to regulate mainly anthocyanin biosynthesis, and *MYB12* could influence the expression of multiple structural genes in both the anthocyanin and flavanol pathways. By contrast, *MYB6*, *bHLH33* and *WD40* were significantly and positively correlated with one another but negatively correlated with the levels of many compounds and most structural genes, indicating that these three transcription factors could regulate together anthocyanin biosynthesis. Our results revealed the information about the temporal and spatial regulation of anthocyanin biosynthesis in *M. hupehensis* and provide the diverse flower color intensities and patterning in Chinese crabapple.

Keywords Crabapple · Cyanidin-3-galactoside · Floral color · MYB

1 Introduction

Flower color is an important property of higher plants. In addition to providing ornamental value, flower color also attracts many insect and avian pollinators. Anthocyanins are the most important floral pigments and contribute to the wide range of red to purple colors (Iwashina 2015). The anthocyanin biosynthesis pathway has been well described in many horticultural species, such as apples, roses and petunias (Peng and Moriguchi 2013; Liu et al. 2015; Li et al. 2018). This pathway involves a number of reactions that are catalyzed by various enzymes. These include phenylalanine ammonia lyase (PAL), chalcone synthase (CHS), chalcone isomerase (CHI), flavanone-3-hydroxylase (F3H), flavanone 3′-hydroxylase (F3′H), dihydroflavonol 4-reductase (DFR), anthocyanin synthase (ANS) and flavonoid-3-*O*-glucosyltransferase (UFGT), as well as side-branching enzymes such as flavonol synthase (FLS), anthocyanin reductase (ANR) and leucoanthocyanidin reductase (LAR) (Liu et al. 2018). It is proven by many authors that transcription factors are regulating anthocyanin biosynthesis pathway, such as R2R3-MYB, basic helix–loop–helix (bHLH) and WD40-repeat (WD40) (Zhao et al. 2013; Liu et al. 2015). These transcription factors activate or suppress the transcription

Electronic supplementary material The online version of this article (https://doi.org/10.1007/s40415-020-00590-y) contains supplementary material, which is available to authorized users.

✉ Houhua Li
lihouhua73@163.com

[1] Institute of Ornamental Plants, College of Landscape Architecture and Art, Northwest A&F University, Yangling 712100, China

and expression of target genes by binding to specific DNA sequences and affecting protein–protein interactions, thereby regulating anthocyanin biosynthesis (Yue et al. 2019). Many studies have shown that the MYB transcription factors primarily regulate flavonoid pathway genes, while bHLH and WD40 transcription factors play roles in the anthocyanin biosynthesis pathway by binding to MYB transcription factors (Zhao et al. 2013; Liu et al. 2015).

Malus hupehensis (Pamp.) Rehder, a member of the *Rosaceae* family, is an important native species in China (Ran et al. 2014). *M. hupehensis* has luxuriant and fragrant flowers. Its petals are red at early flowering stages and then gradually fade to white during flower development (Fig. 1). The fading of floral color is a common phenomenon in ornamental plants, including *Malus* spp. (Zhang et al. 2017), *Lycoris longituba* Lycoris radiata Herb. (Yue et al. 2019) and *Silene littorea* Silene littorea Brot. (Casimiro-Soriguer et al. 2016). The loss of floral anthocyanins results in producing white flowers (Zhao and Tao 2015), but the biochemical and molecular basis for this change remains elusive. *M. hupehensis* is proposed as a model flower to study mechanisms of color fading because of its various merits with regard to phenotype.

In this study, the compositions and concentrations of compounds related to anthocyanin biosynthesis in *M. hupehensis* petals were determined. The expression levels of corresponding genes in the anthocyanin biosynthesis pathway were also analyzed. The mechanism of flower color fading investigated at the chemical and molecular levels provides a theoretical basis for the flower color breeding in *Malus* spp.

2 Material and methods

Plant materials and phenotypic characterization – *Malus hupehensis* was grown in the crabapple resource nursery of Northwest A&F University, Yangling, China. Flowers were randomly collected at five developmental stages from healthy, approximately uniform eight-year-old trees in April, 2018. Sepals, pistils and stamens were quickly removed, and only the petals were collected and stored at − 80 °C. The petals for extracting pigment were vacuum freeze-dried at − 60 °C for 48 h, then ground to powder and stored in airtight containers. Flower developmental stages of *M. hupehensis* were described: stage 1 (S1): small-bud stage; S2: big-bud stage; S3: initial-flowering stage; S4: full-flowering stage and S5: flower-wilting stage (Fig. 1).

Fig. 1 Different flowering stages of *M. hupehensis*: S1: small-bud stage; S2: big-bud stage; S3: initial-flowering stage; S4: full-flowering stage; S5: flower-wilting stage (similarly hereinafter). Different letters between different flower development stages denote significant differences (Duncan test, $p < 0.05$)

Color indices and pH value measurements – The colors of the fresh petals were measured based on the Royal Horticultural Society Color Chart (RHSCC) with a CR-400 chroma meter (Konica Minolta, Tokyo, Japan). Flower color was described using two parameters, L^* (lightness) and a^* (ratio of red to green) (Li et al. 2018). Ten sets of values were obtained and used to calculate means.

The pH value of petal tissue was determined using the method reported by Verweij et al. (2008) with slight modifications. A 0.1 g sample of fresh petal tissue was ground in liquid nitrogen and dissolved in 6 mL of distilled water. The pH value of extract was measured using a ST2011 pH meter (Ohaus Corporation, Shanghai, China). Three biological replicates were performed, and each replicate was measured three times.

Pigment extraction – 0.5 g of powder was added to 25 mL of methanol and incubated in an ultrasound bath at 25 °C for 30 min; this process was repeated three times. The supernatants were pooled and concentrated by rotary flash evaporation until a volume of 25 mL was achieved. The samples were stored at − 20 °C until further analysis. All experiments were performed in triplicate.

Total flavonoid content determination – Total flavonoid content was determined using the aluminum chloride method (Wolfe et al. 2003) with slight modifications. Firstly, 1.0 mL of petal extract was mixed with 0.3 mL of 0.5 mol L^{-1} $NaNO_2$ solution and the mixture was incubated in the dark at room temperature for 5 min. Next, 0.3 mL of 0.3 mol L^{-1} $AlCl_3$ solution was added and the mixture was again incubated in the dark for 5 min. Then, 2.0 mL of 1.0 mol L^{-1} NaOH was added, and the mixture was incubated for 2 min. Finally, 6.4 mL of 30% ethanol was added, and the absorbance at 506 nm was measured using a GENSYS-10S UV spectrophotometry (Thermo, USA). Rutin was used to determine the standard curve, and the results were expressed as milligrams of rutin equivalent (RE) per gram of dry weight (mg RE kg^{-1} DW).

HPLC–DAD analysis – The petal extracts were filtered through a 0.45-μm filter and analyzed by HPLC coupled with a diode array detector (DAD). HPLC–DAD analysis was carried out using a Shimadzu LC-2030C Liquid Chromatograph

(Shimadzu, Kyoto, Japan) equipped with an Inertsil C-18 column (5.0 µm particle size, 4.6 mm × 250 mm). HPLC–DAD separation was performed using a linear gradient of A (0.04% formic acid dissolved in water) and B (acetonitrile) solutions at 40 °C with a flow rate of 0.5 mL min^{-1}. The solvent gradient was as follows: 0 min, 95% A/5% B; 40 min, 60% A/40% B; 45 min, 100% A/0% B, for 15 min. The post-run time was 10 min. Anthocyanin-related compounds were identified by comparing retention times and UV spectral data with authentic standards. The concentration of individual compound was calculated based on peak area and calibration curves derived from corresponding standards. Authentic standards were chosen based on the LC-MC and NMR spectroscopic results from *Malus* spp. and *M. hupehensis* (Li et al. 2007; Wang et al. 2013; Hu et al. 2017), including cyanidin-3-galactoside, cyanidin-3-rutinoside, cyanidin-3-arabinoside, cyanidin-3-glucoside, catechin, chlorogenic acid, ferulic acid, caffeic acid, epicatechin, proanthocyanidin B1, proanthocyanidin B2, rutin, hyperoside, dihydroquercetin, phlorizin and quercetin from Shanghai Yuanye Biological Company.

Quantitative real-time PCR – RNA extraction was performed using an E.Z.N.A Plant RNA Kit (Omega, USA) extraction kit. First-strand cDNA was synthesized from 1 ng of RNA by reverse transcription according to the manual of the PrimeScriptTM RT reagent kit with gDNA Eraser kit (TaKaRa, Japan). Quantitative real-time PCR was performed on a real-time PCR instrument (Applied Biosystems, CA, USA). SYBR® Premix Ex Taq TM (TaKaRa, Japan) was used according to the manufacturer's instructions with three technical replicates and three biological replicates. Data analysis was performed using the $2^{-\Delta\Delta CT}$ method with 18S ribosomal RNA that was used as the reference gene (Tian et al. 2017). All primers tested are shown in Table S1.

Statistical analysis – To further examine the major compounds that influence flower color formation, the total contents of different kinds of compounds were calculated based on the concentrations of single compounds determined by HPLC–DAD. The ratio of Sn/S5 was obtained based on the total contents of compounds at five different developmental stages, where "Sn" refers to S1, S2, S3, S4 or S5. All statistical analyses were carried out using SPSS 20.0 software. All the data are shown as mean values ± SD. A one-way analysis of variance (ANOVA) was used to detect the significant differences for each experimental test condition, and $P < 0.05$ was considered statistically significant.

3 Results

Color indices and pH value – The flower color of *M. hupehensis* changes gradually during development. The flower bud showed no red when it is wrapped by the sepals (S1). The petal color changes quickly to red when the buds are exposed to light (S2). Later, the flower color gradually fades to white. Therefore, petals are the reddest at S2 (Fig. 1). Color differences among petals were determined based on their L^* and a^* values. In the uniform color space, lightness increases as L^* value increases from 0 to 100. Negative values of a^* indicate green, whereas positive values of a^* indicate red. The results showed that the L^* value of *M. hupehensis* petals gradually increased over time. The a^* value initially increased and then decreased; the highest a^* values occurred at S2 (Table 1), consistent with the observed changes in flower color.

The pH value of petal extracts was determined to assess the influence of pH on flower color. The pH values varied from 5.48 to 5.75, and the lowest value occurred at S2. However, the pH value did not differ significantly among the five stages (Table 1). These results indicated that pH value of petal has only a slight influence on flower color in *M. hupehensis*.

Total flavonoid content – The total flavonoid content of petals was measured using the aluminum chloride method. Total flavonoid content increased initially and then decreased; it varied from 48,753.39 to 72,479.67 mg RE kg^{-1} DW at different stages (Table 2). The highest content occurred at S2, when total flavonoid content was 1.5 times higher than the lowest content (S5).

Composition of flavonoids – The components and concentrations of flavonoids in *M. hupehensis* petal extracts (Table 3), three anthocyanins, including cyanidin-3-galactoside, cyanidin-3-arabinoside and cyanidin-3-rutinoside, were detected in *M. hupehensis* petals at whole flower development. Of these, cyanidin-3-galactoside was the major

Table 1 Color indices and pH values of *M. hupehensis* flower at five flowering stages

Stages	L^*	a^*	pH
Stage 1	64.77 ± 3.07	-3.91 ± 2.06	5.62 ± 0.02
Stage 2	68.78 ± 5.01	4.09 ± 2.61	5.48 ± 0.02
Stage 3	79.95 ± 3.04	2.26 ± 1.55	5.53 ± 0.04
Stage 4	84.39 ± 2.24	1.72 ± 0.63	5.67 ± 0.03
Stage 5	88.76 ± 2.18	-0.65 ± 0.20	5.75 ± 0.02

The values represented mean ± SD, and different letters between different flower development stages denote significant differences (Duncan test, $P < 0.05$)

Table 2 Total flavonoid contents of *M. hupehensis* flower at five flowering stages

Stages	Total flavonoid content (mg CE kg^{-1} DW)
Stage 1	52,588.08 ± 3,150.95 bc
Stage 2	72,479.67 ± 6,488.42 a
Stage 3	61,327.92 ± 9,221.85 b
Stage 4	57,506.78 ± 6,515.78 b
Stage 5	48,753.39 ± 2,305.75 c

The values represented mean ± SD, and different letters between different flower development stages denote significant differences (Duncan test, $P < 0.05$)

anthocyanin. Its concentration increased firstly and it was 1430.75 mg kg^{-1} DW, a value 10.9 times higher than the lowest content (at S5). The concentration of cyanidin-3-galactoside declined dramatically after S2. Cyanidin-3-arabinoside and cyanidin-3-rutinoside concentrations remained low and there was no significant difference during flower development.

Besides, other flavonoids were detected in petals, including flavonols (rutin, hyperoside and quercetin), flavanols (catechin, epicatechin, procyanidin B1 and procyanidin B2), phenolic acids (chlorogenic acid, ferulic acid and caffeic acid), dihydroflavonols (dihydromyricetin and (+)-dihydroquercetin), and dihydrochalcone (phloridzin). Almost all of the flavonols and total dihydroflavonols reached their highest concentration at S2, with the exception of (+)-dihydroquercetin. Catechin and epicatechin, which were the most abundant of flavanols, achieved their highest value at S2 and S3, respectively. However, after decreasing somewhat, the concentrations of these two compounds showed an uptrend, resulting in an increase in total flavanols. Chlorogenic acid and ferulic acid were the major phenolic acids, and their maximums were detected at S3. Phlorizin peaked at S1 and declined thereafter (Table 3).

To further determine the major compounds that influence flower color formation, the Sn/S5 ratio of various compounds was calculated at different developmental stages. The Sn/S5 ratio of total anthocyanins changed dramatically during flowering development, and the S2/S5 was 6.1 times, the highest ratio of any compounds. Compared with total anthocyanins, the Sn/S5 ratio of total flavonols showed a similar change trend but a lower intensity. The Sn/S5 ratios of total flavanols, phenolic acids, dihydroflavonols and dihydrochalcone showed little change across five stages, although contents of these substances were higher compared

Table 3 Components and concentrations of polyphenols in *M. hupehensis* at five flowering stages/mg kg^{-1} DW

Polyphenol	Stage 1	Stage 2	Stage 3	Stage 4	Stage 5
Total anthocyanin	577.26	1543.76	750.03	327.36	242.44
Cyanidin-3-galactoside	460.22 ± 85.97c	1430.75 ± 30.76a	640.48 ± 38.56b	219.42 ± 25.66d	131.37 ± 15.97d
Cyanidin-3-arabinoside	46.90 ± 0.51b	48.15 ± 0.32b	47.50 ± 0.31b	47.51 ± 1.66b	52.26 ± 1.09a
Cyanidin-3-rutinoside	70.14 ± 1.05a	65.16 ± 0.42b	62.11 ± 0.46c	60.80 ± 0.85d	59.13 ± 0.16e
Total flavonols	11,311.90 ± 2606.84	32,972.17 ± 974.00	26,562.56 ± 5705.29	17,266.78 ± 702.22	11,348.13 ± 2,693.51
Rutin	9130.03 ± 2279.39b	30,191.34 ± 917.23a	25,018.57 ± 5541.40a	16,001.90 ± 683.32b	10,148.15 ± 2588.22b
Hyperoside	1510.87 ± 153.62b	2205.21 ± 657.22a	1205.83 ± 93.71b	1060.55 ± 15.58b	1057.01 ± 78.43b
Quercetin	671.00 ± 175.43b	1204.38 ± 432.59a	338.16 ± 70.30bc	204.33 ± 3.32c	142.97 ± 26.86c
Total flavanols	5922.52 ± 1019.35	9653.89 ± 569.56	9257.01 ± 599.45	5746.18 ± 1718.85	6596.95 ± 773.49
Catechin	68.80 ± 9.65d	2643.51 ± 81.73c	6766.59 ± 480.99a	4524.76 ± 129.64b	3153.98 ± 433.662c
Epicatechin	5579.67 ± 1130.47ab	6904.83 ± 481.12a	2136.58 ± 450.98c	2284.72 ± 53.34bc	3918.99 ± 858.79bc
Procyanidin B1	106.46 ± 1.39a	104.57 ± 5.04a	98.14 ± 0.25b	96.69 ± 2.13b	ND
Procyanidin B2	190.53 ± 7.24	ND	ND	ND	ND
Total phenolic acids	11,376.92 ± 1286.72	21,665.59 ± 1543.06	24,101.60 ± 757.04	17,466.69 ± 2857.20	13,009.19 ± 450.31
Chlorogenic acid	7327.44 ± 866.55c	16,566.44 ± 1407.69a	18,873.14 ± 841.71a	13,163.36 ± 2870.73b	9027.71 ± 654.23c
Ferulic acid	3708.77 ± 442.98c	4608.97 ± 310.25ab	4932.03 ± 86.09a	4033.43 ± 786.15bc	3724.73 ± 223.84c
Caffeic acid	340.71 ± 6.45a	317.25 ± 6.35b	296.42 ± 0.54c	269.90 ± 11.12d	264.57 ± 1.35e
Total dihydroflavonols	798.66 ± 58.72	718.83 ± 76.60	573.60 ± 16.04	571.44 ± 25.86	542.65 ± 24.20
Dihydromyricetin	31.42 ± 9.47b	54.68 ± 2.00a	7.50 ± 0.60c	15.52 ± 0.69bc	33.24 ± 11.51b
(+)-Dihydroquercetin	767.24 ± 67.42a	682.37 ± 60.06b	568.60 ± 16.49c	561.09 ± 11.62c	509.41 ± 12.69c
Total dihydrochalcone	18,641.37 ± 671.09	17,475.09 ± 1,738.26	12,385.23 ± 1,677.90	9,105.57 ± 246.3206	8,204.84 ± 1,582.45
Phlorizin	18,641.37 ± 671.09a	17,475.09 ± 1738.26a	12,385.23 ± 1677.90b	9105.57 ± 246.3206c	8204.84 ± 1582.45c

The values represented mean ± SD. For each row, different letters between different flower development stages denote significant differences (Duncan test, $P < 0.05$)

with total anthocyanins in petals (Fig. 2; Table 3). These results further demonstrate that the decline in total anthocyanin content is the major reason for the flower color fading in *M. hupehensis*.

Expression levels of anthocyanin biosynthesis-related genes – Transcript levels of genes related to anthocyanin biosynthesis were analyzed by qRT-PCR at the five flowering stages of *M. hupehensis*. (Fig. 3). Most structural genes, including *PAL*, *FHT*, *CHS*, *CHI*, *FHT*, *DFR*, *FLS*, *ANS* and *UFGT*, followed a consistent expression pattern whereby their transcripts levels increased markedly, reached a maximum at S2 and sharply decreased thereafter. Expression of *PAL*, *ANS*, *FLS* and *CHS* showed striking differences during the flowering development, and their relative expression levels at S2 compared with S5 were 285.33, 100.12, 67.77 and 42.94, respectively. The transcript levels of *ANR* and *LAR* peaked at S2 and S3, respectively, and slightly increased after decreasing somewhat. These two genes can catalyze the transformation of anthocyanidins and anthocyanins to flavanols, and their transcription profiles were similar to the pattern of total flavanols content (Fig. 3).

The expression levels of multiple transcription factors at different flowering stages were also determined. *MYB12* expressions differed significantly among the five stages and reached a maximum at S3 that was 28.1-fold higher than that at S5. There was no significant difference in *MYB12* expression between S2 and S3. *MYB10* expression reached its highest level at S2 and decreased thereafter. The expression of *MYB6* decreased initially, reached a minimum at S2 and then increased. The expression profiles of *WD40* and *bHLH33* were similar to that of *MYB6* (Fig. 4).

Correlation of flavonoids and genes – Correlation analyses were performed to investigate the relationship between the anthocyanin biosynthesis-related compounds and gene expression during flower development. Total anthocyanins level was significantly positively correlated with the expression of *PAL*, *CHI*, *CHS*, *FLS*, *DFR*, *ANS*, *MYB10* and *MYB12*, but negatively correlated with the expression of *MYB6*, *bHLH33 a*nd *WD40*. Moreover, the strongest relationship (0.903**) was observed between total anthocyanins and *ANS*. Also, total flavonols and flavanols content were positively correlated with the expression of *CHS*, *CHI*, *DFR*, *LAR*, *MYB10* and *MYB12*.

MYB10 expression was significantly correlated with that of *CHS*, *CHI*, *DFR* and *ANS*. Large correlations were observed between *MYB12* and the structural genes *CHI*, *CHS*, *F3H*, *F3'H*, *DFR* and *LAR*. By contrast, *MYB6*, *bHLH33* and *WD40* expression was negatively correlated with the levels of many compounds and expression of most structural genes. The expression levels of these three transcription factors were significantly positively correlated with one another. (Fig. 5).

4 Discussion

Malus hupehensis flower is red during early stages and fade to white during flower development. Anthocyanins are the key pigmentation molecules in *Malus* petals (Jiang et al. 2014; Rehman et al. 2017). In this study, abundant anthocyanin biosynthesis-related compounds were detected in the petals of *M. hupehensis*. Of these compounds, cyanidin-3-galactoside was the major anthocyanin. Total anthocyanin contents changed dramatically as petal color changed. The expression level of anthocyanin biosynthesis-related genes (*PAL*, *CHS*, *CHI*, *DFR*, *FLS*, *ANS* and *UFGT*) were initially elevated, peaked at S2 and declined afterward, coincident with a change in a^* value that reflected fading trends of flower color. The results suggest that these genes play important roles in regulating anthocyanin biosynthesis. In particular, *ANS* expression was strongly correlated with total

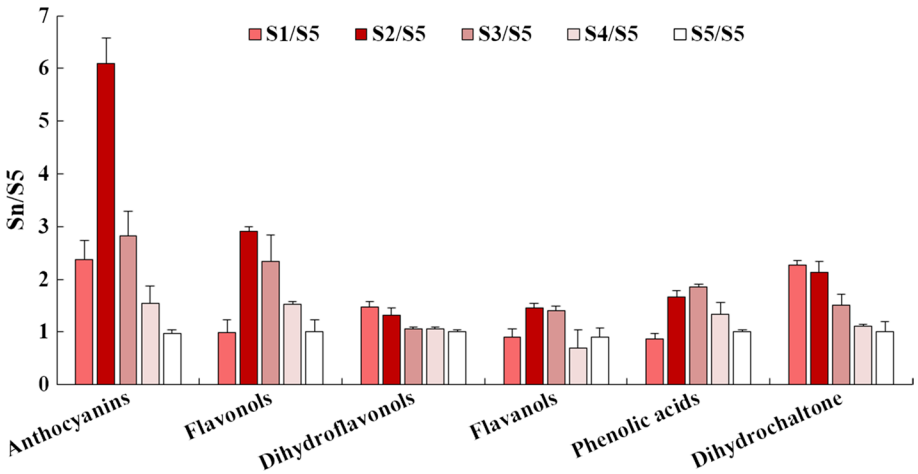

Fig. 2 The ratio (Sn/S5) of contents of flavonoids in petals of *M. hupehensis*

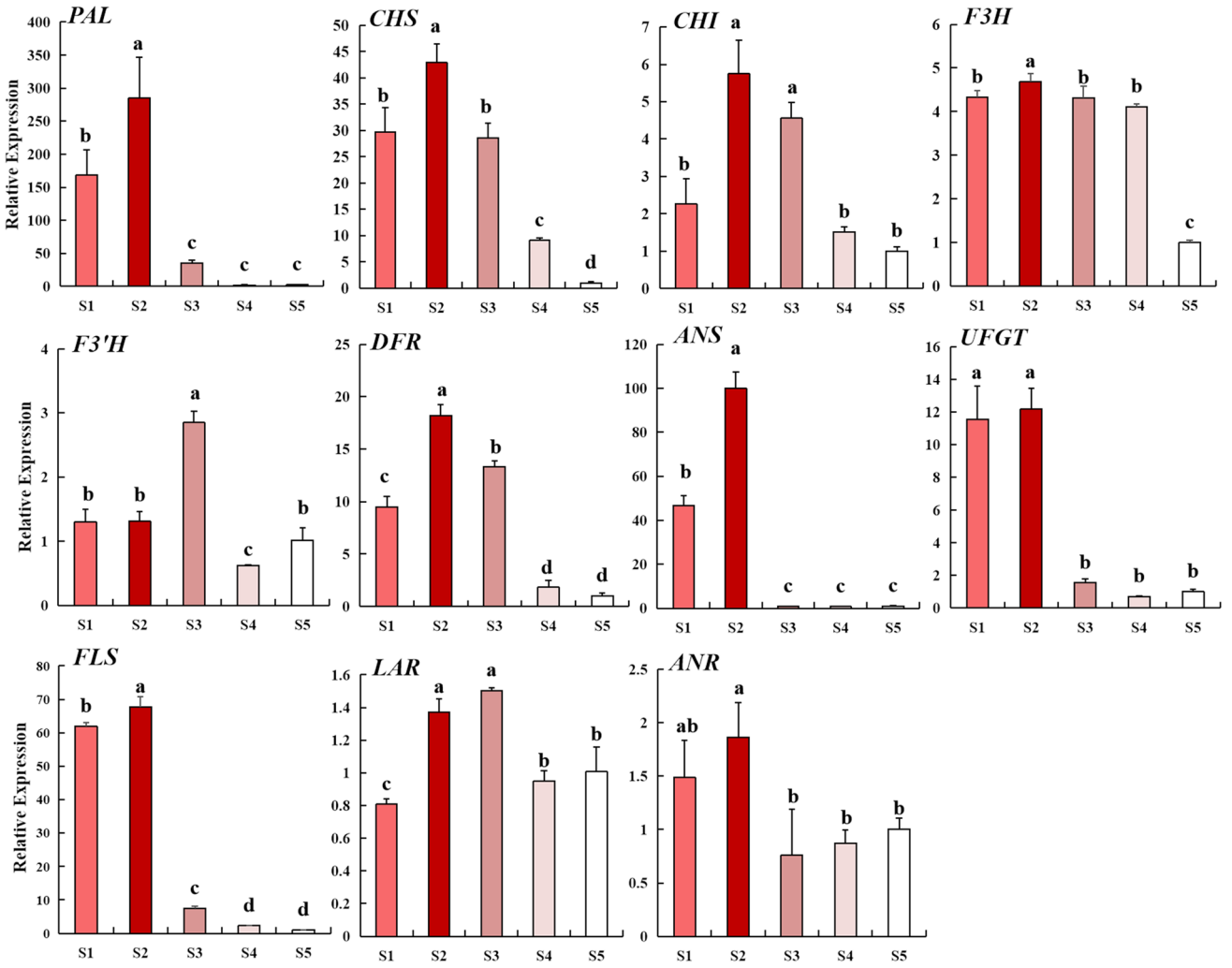

Fig. 3 Relative expression of structural genes in anthocyanin synthesis pathway in *M. hupehensis* during different flower development stages. Different letters between different flower development stages denote significant differences (Duncan test, $P < 0.05$)

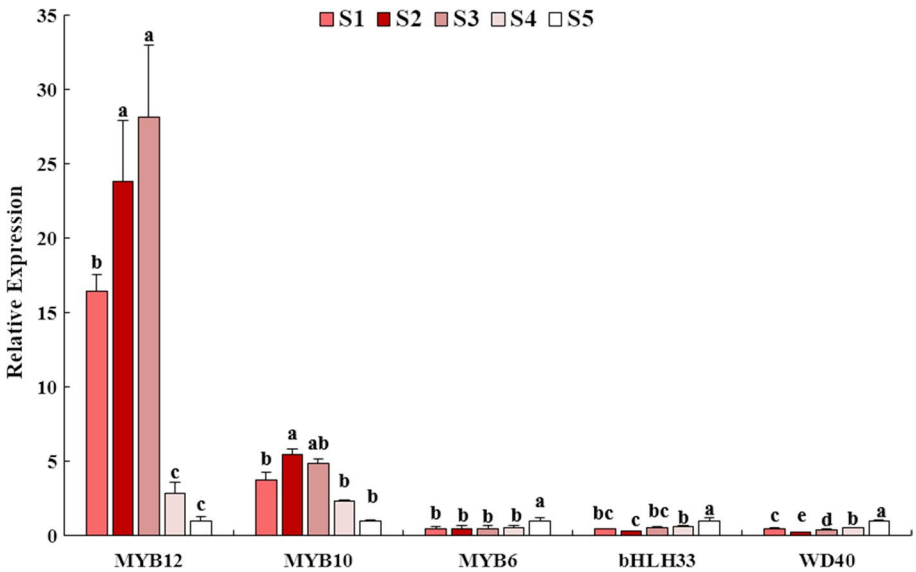

Fig. 4 Relative expression of transcription factors in anthocyanin synthesis pathway in *M. hupehensis* during different development stages. Different letters between different flower development stages denote significant differences (Duncan test, $P < 0.05$)

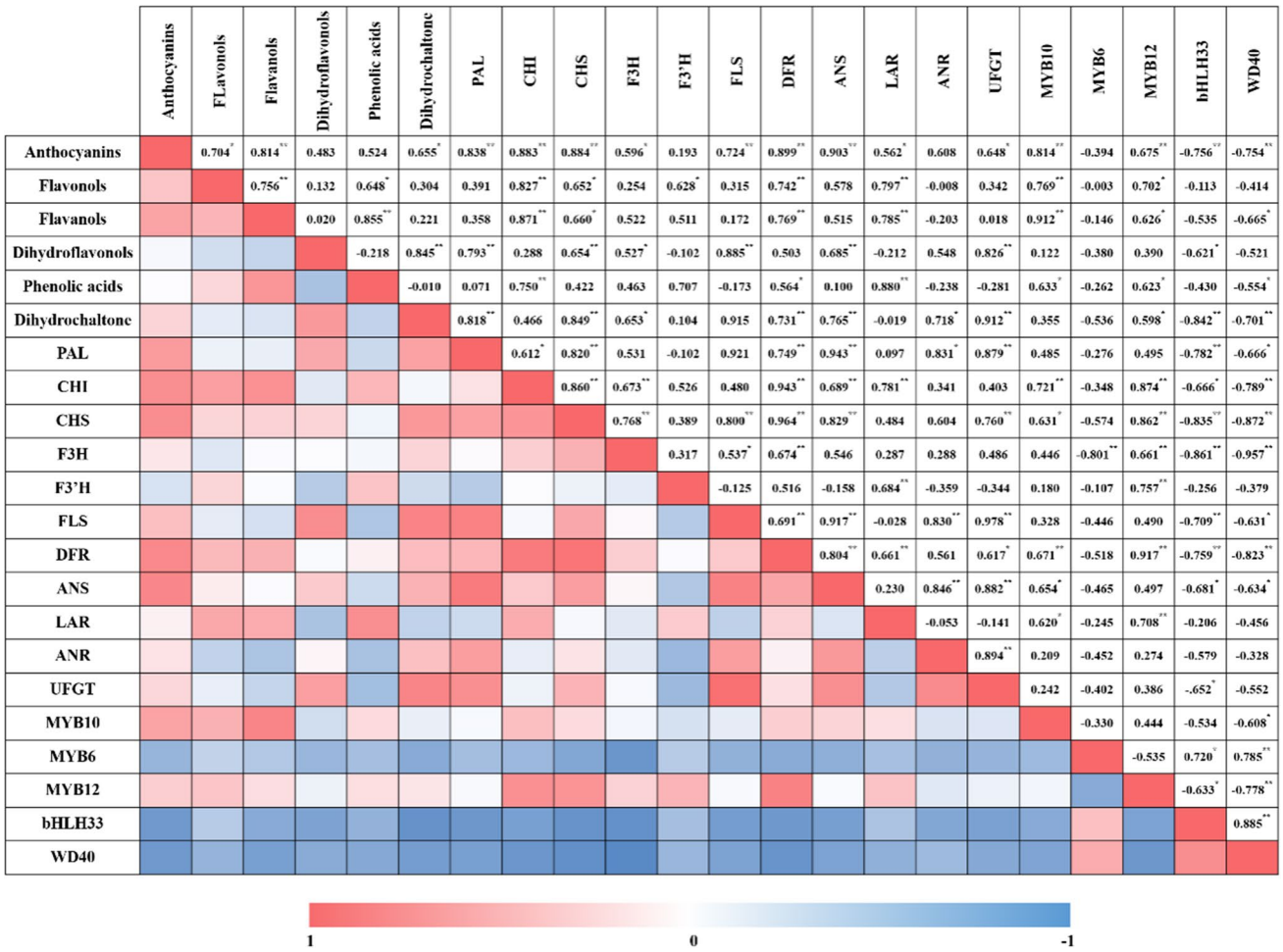

Fig. 5 The Pearson correlation analysis between anthocyanin biosynthesis-related gene expressions and flavonoids contents in petals of *M. hupehensis*. *Indicates significant correlation at $P < 0.05$, and **indicates extremely significant correlation at $P < 0.01$

anthocyanins and appeared to play a principal role in the anthocyanin accumulation of *M. hupehensis*.

As one of the largest families of transcription factors in the regulatory network of anthocyanin biosynthesis pathways, MYBs participate in a very complex regulation process. (Liu et al. 2015). In *Malus* species, *MdMYB10* regulates anthocyanin biosynthesis by directly binding to the *DFR* promoters in apple (Espley et al. 2007, 2013), and *McMYB10* positively regulates *McF3'H* by directly binding to promoter motifs in crabapple leaves. In this study, the expression of *MYB10* that was significantly correlated with that of structural genes (*CHS*, *CHI*, *DFR*, *ANS*) suggested that *MYB10* regulates anthocyanin biosynthesis by means of influencing expressions of these genes in flowers. In addition to *MYB10*, high expression levels of *MYB12* were observed in flowers, and a strong correlation was observed between expression of *MYB12* and that of *CHS*, *CHI*, *DFR*, *F3H*, *F3'H* and *LAR* (a key gene of flavanol synthesis). These results indicated that *MYB12* may have wide ranging influence on the expression of structural genes not only of anthocyanin synthesis, but also of flavanol in *M. hupehensis* flower. *MYB12* isolated from leaves co-regulated anthocyanin and flavanol biosynthesis (Tian et al. 2017), and *MYB12* from fruits mainly regulated flavanol by affecting the promoter activity of *LAR* (Wang et al. 2017). These researches demonstrate that the same transcription factors can have varied functions in different tissues and species, despite the fact that their sequences are highly conserved. In brief, both of *MYB12* and *MYB10* appear to promote anthocyanin accumulation in flowers by different regulatory mechanisms.

MdMYB6 is a repressor of anthocyanin accumulation in *Malus*, and *MdMYB6* over-expression in Arabidopsis decreased anthocyanin content and down-regulated the expression of corresponding biosynthesis genes (Gao et al. 2011). In this study, the pattern of *MYB6* expression was opposite to that of most structural genes as well as that of *MYB10* and *MYB12*, consistent with the reports mentioned above. In most previous studies, bHLH33 interacted with

transcriptional activators (like MYB12 and MYB10) to promote anthocyanin biosynthesis (Espley et al. 2007; Wang et al. 2017). In our study, the expression pattern of *bHLH33* was opposite to that of *MYB10* or *MYB12*, but *bHLH33* expression was significantly and positively correlated with that of *MYB6*. It has been reported that MYB16 in apple, which is a transcriptional repressor like MYB6, repressed anthocyanin synthesis; however, its inhibition effect was weakened when it interacted with bHLH33 (Xu et al. 2017). In sweet cherry, a bHLH33 closely homologous to bHLH33 in apple strongly inhibited anthocyanin biosynthesis (Starkevič et al. 2015). These researches demonstrate that bHLH33 could interact with multiple MYBs and play variable roles in the anthocyanin biosynthesis pathway in diverse plants. Our results suggested that bHLH33 may interact with MYB6 to regulate anthocyanin biosynthesis; whether it intensifies or suppresses the effect of MYB6 requires further study.

WD40 in apple influences structural gene expressions in the anthocyanin biosynthesis pathway by interacting with bHLHs (such as bHLH33 and bHLH3) (An et al. 2012). In our study, the expression levels of *bHLH33* and *WD40* were significantly and positively correlated. These results indicate that WD40 may interact with bHLH33 to form a MBW complex with MYB6 to regulate anthocyanin biosynthesis. These results suggest a new researching direction to confirm the interaction among MYB6, bHLH33 and WD40 with additional experiment (such as electromobility shift assays and yeast two hybrid assays).

In conclusion, our study demonstrated that the flower color fading of *M. hupehensis* resulted from anthocyanin biosynthesis blocked by corresponding structural genes whose expressions were down-regulated during developmental process. The expression of several transcription factor (MYB12, MYB10 and MYB6) appeared to have a significant effect on the expression of structural genes related to anthocyanin biosynthesis. In particular, the bHLH33 and WD40 may have specific function in flower color formation. This study proposes a mechanism for flower color fading in *M. hupehensis* and provides a basis for further research on floral color formation.

Acknowledgements This work was supported by the National Natural Science Foundation of China [31570697].

Authors' Contributions The experiments were conceived and designed by Houhua Li. The experiments were carried out by Meiling Han, Chen Yang, Jiaxin Meng and Ting Shen. The data were analyzed by Meiling Han and Chen Yang. Meiling Han, Jing Zhou and Jiabin Zhu drafted the manuscript and gathered figures. Jiaxin Meng, Zhuanxia Xin, Ting Shen and Jiabin Zhu participated in the design of experiments and edited the manuscript. All authors read, edited and approved the manuscript.

References

An XH, Tian Y, Chen KQ, Wang XF, Hao YJ (2012) The apple WD40 protein MDTTG1 interacts with bHLH but not MYB proteins to regulate anthocyanin accumulation. J Plant Physiol 169:710–717. https://doi.org/10.1016/j.jplph.2012.01.015

Casimiro-Soriguer I, Eduardo N, Buide ML, del Valle JC, Whittall JB (2016) Transcriptome and biochemical analysis of a flower color polymorphism in *Silene littorea* (Caryophyllaceae). Front Plant Sci. https://doi.org/10.3389/fpls.2016.00204

Espley R, Hellens R, Putterill J, Stevenson D, Kutty-Amma S, Allan A (2007) Red colouration in apple fruit is due to the activity of the MYB transcription factor, MdMYB10. Plant J 49:414–427. https://doi.org/10.1111/j.1365-313x.2006.02964.x

Espley RV, Bovy A, Bava C et al (2013) Analysis of genetically modified red-fleshed apples reveals effects on growth and consumer attributes. Plant Biotechnol J 11:408–419. https://doi.org/10.1111/pbi.12017

Gao J, Shen X, Zhang Z, Peng RH, Xiong A, Xu J, Yao Q (2011) The MYB transcription factor *MdMYB6* suppresses anthocyanin biosynthesis in transgenic Arabidopsis. Plant Cell Tissue Organ Cult 106:235–242. https://doi.org/10.1007/s11240-010-9912-9914

Hu Q, Chen Y, Jiao Q, Khan A, Shan J, Cao G, Li F, Zhang C, Lou H (2017) Polyphenolic compounds from *Malus hupehensis* and their free radical scavenging effects. Nat Prod Res 32:1–7. https://doi.org/10.1080/14786419.2017.1367784

Iwashina T (2015) Contribution to flower colors of flavonoids including anthocyanins: a review. Nat Prod Commun 10:529–544. https://doi.org/10.1177/1934578x1501000335

Jiang R, Tian J, Song T, Zhang J, Yao Y (2014) The *Malus* crabapple transcription factor McMYB10 regulates anthocyanin biosynthesis during petal coloration. Sci Hortic 166:42–49. https://doi.org/10.1016/j.scienta.2013.12.002

Li HH, Flachowsky H, Fischer TC, Hanke MV, Forkmann G, Treutter D, Schwab W, Hovmann T, Szankowski I (2007) Maize *lc* transcription factor enhances biosynthesis of anthocyanins, distinct proanthocyanidins and phenylpropanoids in apple (*Malus domestica* Borkh.). Planta 226:1243–1254. https://doi.org/10.2307/23389811

Li Z, Zhao M, Jin J, Zhao L, Xu Z (2018) Anthocyanins and their biosynthetic genes in three novel-colored *Rosa rugosa* cultivars and their parents. Plant Physiol Biochem 129:421–428. https://doi.org/10.1016/j.plaphy.2018.06.028

Liu J, Osbourn A, Ma P (2015) MYB transcription factors as regulators of phenylpropanoid metabolism in plants. Mol Plant 8:689–708. https://doi.org/10.1016/j.scienta.2013.12.002

Liu Y, Tikunov Y, Schouten RE, Marcelis LFM, Visser RGF, Bovy A (2018) Anthocyanin biosynthesis and degradation mechanisms in *Solanaceous* vegetables: a review. Front Chem. https://doi.org/10.3389/fchem.2018.00052

Peng T, Moriguchi T (2013) The molecular network regulating the coloration in apple. Sci Hortic 163:1–9. https://doi.org/10.1016/j.scienta.2013.06.005

Ran K, Yang H, Sun X, Li Q, Jiang Q, Zhang W, Shen W (2014) Isolation, characterization, and structure analysis of a vacuolar processing enzyme gene (MhVPEγ) from *Malus hupehensis* (Pamp) Rehd. Appl Biochem Biotechnol 173:579–595. https://doi.org/10.1007/s12010-014-0867-5

Rehman R, You Y, Yang C, Khan AR, Li P, Ma F (2017) Characterization of phenolic compounds and active anthocyanin degradation in crabapple (*Malus orientalis*) flowers. Hortic Environ Biotechnol 58:324–333. https://doi.org/10.1007/s13580-018-0001-7

Starkevič P, Paukštytė J, Kazanavičiūtė V, Denkovskienė E, Stanys V, Bendokas V, Šikšnianas T, Ražanskienė A (2015) Expression and anthocyanin biosynthesis modulating potential of sweet cherry

(*Prunus avium* L.) MYB10 and bHLH genes. PLoS ONE. https://doi.org/10.1371/journal.pone.0126991

Tian J, Zhang J, Han Z, Song T, Li J, Wang Y, Yao Y (2017) McMYB12 transcription factors co-regulate proanthocyanidin and anthocyanin biosynthesis in *Malus* crabapple. Sci Rep. https://doi.org/10.1038/srep43715

Verweij W, Spelt C, Di Sansebastiano GP, Vermeer J, Reale L, Ferranti F, Koes R, Quattrocchio F (2008) An H^+ P-ATPase on the tonoplast determines vacuolar pH and flower colour. Nat Cell Biol 10:1456–1462. https://doi.org/10.1038/ncb1805

Wang S, Zhu X, Wang X, Shen T, Xiang F, Lou H (2013) Flavonoids from *Malus hupehensis* and their cardioprotective effects against doxorubicin-induced toxicity in H9c2 cells. Phytochemistry 87:119–125. https://doi.org/10.1016/j.phytochem.2012.11.020

Wang N, Xu H, Jiang S, Zhang Z, Lu N, Qiu H, Qu C, Wang Y, Wu S, Chen X (2017) MYB12 and MYB22 play essential roles in proanthocyanidin and flavonol synthesis in red-fleshed apple (*Malus sieversii* f. *niedzwetzkyana*). Plant J 90:276–292. https://doi.org/10.1111/tpj.13487

Wolfe K, Wu XZ, Rui HL (2003) Antioxidant activity of apple peels. J Agric Food Chem 51:609–614. https://doi.org/10.1021/jf020782a

Xu H, Wang N, Liu J, Qu C, Wang Y, Jiang S, Lu N, Wang D, Zhang Z, Chen X (2017) The molecular mechanism underlying anthocyanin metabolism in apple using the MdMYB16 and MdbHLH33 genes. Plant Mol Biol 94:149–165. https://doi.org/10.1007/s11103-017-0601-0

Yue Y, Liu J, Shi T, Chen M, Li Y, Du J, Jiang H, Yang X, Hu H, Wang L (2019) Integrating transcriptomic and GC-MS metabolomic analysis to characterize color and aroma formation during tepal development in *Lycoris longituba*. Plants. https://doi.org/10.3390/plants8030053

Zhang J, Liu Y, Bu Y, Zhang X, Yao Y (2017) Factor analysis of MYB gene expression and flavonoid affecting petal color in three crabapple cultivars. Front Plant Sci. https://doi.org/10.3389/fpls.2017.00137

Zhao D, Tao J (2015) Recent advances on the development and regulation of flower color in ornamental plants. Front Plant Sci 6:261. https://doi.org/10.3389/fpls.2015.00261

Zhao L, Gao L, Wang H, Chen X, Wang Y, Yang H, Wei C, Wan X, Xia T (2013) The R2R3-MYB, bHLH, WD40, and related transcription factors in flavonoid biosynthesis. Funct Integr Genom 13:75–98. https://doi.org/10.1007/s10142-012-0301-4